A voltage-dependent gap junction in *Drosophila melanogaster*

Vytas K. Verselis, Michael V. L. Bennett, and Thaddeus A. Bargiello
Albert Einstein College of Medicine, Bronx, New York 10461 USA

ABSTRACT Steady-state and kinetic analyses of gap junctional conductance, g_j, in salivary glands of *Drosophila melanogaster* third instar larvae reveal a strong and complex voltage dependence that can be elicited by two types of voltages. Voltages applied between the cells, i.e., transjunctional voltages, V_j, and those applied between the cytoplasm and the extracellular space, inside-outside voltages, $V_{i,o}$, markedly alter g_j. Alteration of V_{i-o} while holding $V_j = 0$, i.e., by equal displacement of the voltages in the cells, causes g_j to increase to a maximum on hyperpolarization and to decrease to near zero on depolarization. These conductance changes associated with V_{i-o} are fit by a model in which there are two independent gates in series, one in each membrane, where each gate is equally sensitive to V_{i-o} and exhibits first order kinetics. V_j's generated by applying voltage steps of either polarity to either cell, substantially reduce g_j. These conductance changes exhibit complex kinetics that depend on V_{i-o} as well as V_j. At more positive V_{i-o}'s, the changes in g_j have two phases, an early phase consisting of a decrease in g_j for either polarity of V_j and a later phase consisting of an increase in g_j on hyperpolarizing either cell and a decrease on depolarizing either cell. At negative V_{i-o}'s in the plateau region of the g_j–V_{i-o} relation, the later slow increase in g_j is absent on hyperpolarizing either cell. Also, the early decrease in g_j for either polarity of V_j is faster the more positive the V_{i-o}. The complex time course elicited by applying voltage steps to one cell can be explained as combined actions of V_{i-o} and V_j, with the early phase ascribable to V_j, but influenced by V_{i-o}, and the later phase to the changes in V_{i-o} associated with the generation of V_j. The substantially different kinetics and sensitivity of changes in g_j by V_{i-o} and V_j suggests that the mechanisms of gating by these two voltages are different. Evidently, these gap-junction channels are capable of two distinct, but interactive forms of voltage dependence.

INTRODUCTION

Gap junctions mediate intercellular chemical and electrical communication in a wide variety of tissues. In some cells, gap junctional conductance, g_j, exhibits a strong dependence on voltage (Spray et al., 1981; Obaid et al., 1983; see also Spray et al., 1985) with sensitivities, expressed in terms of equivalent charge movement, comparable to those for ion channels in excitable membranes (Hille, 1984). However, analyses of cloned cDNA sequences from several vertebrate tissues (Paul, 1986; Kumar and Gilula, 1986; Beyer et al., 1987; Gimlich et al., 1988; Ebihara et al., 1989; Zhang and Nicholson, 1989) indicate that gap junction proteins (connexins) are unrelated to the family of voltage-sensitive ion channels that include those selective for Na^+, K^+, and Ca^{++} (see Caterall, 1988). In particular there is no obvious homologue or analogue of the S4 domain to which voltage sensitivity of activation is ascribed (Stuhmer et al., 1989). Furthermore, whereas ion channels that span a single membrane are sensitive to changes in the transmembrane voltage, gap-junction channels can be sensitive to two different voltages, the voltage difference between the cells, transjunctional voltage, V_j, and the voltage between the cytoplasm or channel interior and the extracellular space, inside-outside voltage, V_{i-o}.

These two types of voltage dependence are possible because of the distinctive structure of the gap-junction channel, which consists of two hemichannels, one in each membrane of two cells in close apposition. The hemichannels are joined at the center of the intercellular gap between the cells (Makowski et al., 1977; Unwin and Zampighi, 1980). In the case of a coupled cell pair, gating by V_{i-o} could be induced by displacing the voltage in both cells equally. This voltage would be developed across the channel macromolecule between both the cytoplasm and lumen of the channel and the extracellular space (Fig. 1). The high coupling coefficients possible between well coupled cells indicates that there is little leakage from gap-junction channels into the extracellular space (Bennett, 1977) so that V_{i-o} would essentially be uniform along the channel. When the voltages in the two cells are made unequal to establish V_j, then V_{i-o} would again be developed except that it would be nonuniform along the channel. Thus, placing cells at unequal potentials necessarily imposes both V_{i-o} and V_j. If only V_j sensitivity were present, the effect on g_j would be independent of the cell potentials from which V_j was

Address correspondence to Dr. Vytas K. Verselis.

0006-3495/91/01/114/13 $2.00

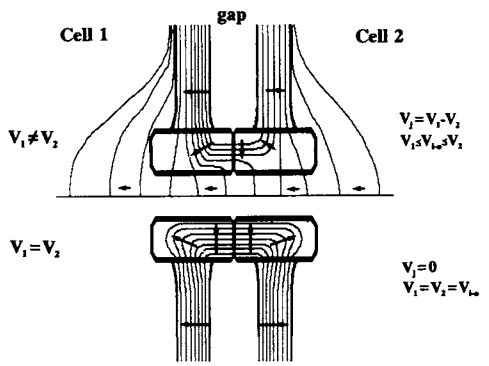

FIGURE 1 Diagram of a gap-junction channel showing presumed isopotential lines in the presence of a resting potential (V_{i-o}) and no V_j (*lower half*) and when both V_{i-o} and V_j are present (*upper half*). Arrows indicate field direction and suggest approximate magnitude.

generated and the same effect would result from hyperpolarization or depolarization of either cell.

Gap junctional voltage dependence, whether to V_j or V_{i-o}, varies among tissues in time course, sensitivity, and dependence on polarity. In certain electrical synapses of crayfish and hatchetfish, g_j rectifies and is much greater for the presynaptic cell positive relative to the postsynaptic cell (Furshpan and Potter, 1959; Auerbach and Bennett, 1969; Margiotta and Walcott, 1982). Rectification is very fast (<0.2 ms) as would be required for impulse transmission and appears to be solely dependent on V_j (Giaume and Korn, 1985; Jaslove and Brink, 1986). In amphibian and tunicate embryos, V_j of either polarity strongly reduces g_j (Spray et al., 1981; Knier and Bennett, 1985), with symmetric reduction in g_j around $V_j = 0$. Conductance changes are slow compared to many voltage-gated channels and time constants to reach steady state are in the range of tens to hundreds of milliseconds. These symmetrically V_j-dependent junctions also show little or no sensitivity to V_{i-o} and the same changes in g_j are produced by equal depolarizing and hyperpolarizing steps applied to either cell. In *Chironomus* salivary glands, g_j is strongly dependent on V_{i-o} with g_j reduced by equal depolarization of cells, i.e., with V_j maintained at zero (Obaid et al., 1983). Although the *Chironomus* junctions were reported to be unaffected by V_j, some dependence on V_j is present in the data presented by these authors. Gap junctions between rat neonatal cardiac myocytes (Rook et al., 1988), rat hepatocytes (Spray et al., 1990) and *Xenopus* oocytes expressed from connexin 32 or 26 cRNA (Barrio et al., 1990) were more recently reported to display voltage dependence of the transjunctional type. Gap junctions in many other preparations have little if any voltage dependence, including crayfish (Johnston and Ramon, 1982) and earthworm septate axons (Verselis and Brink, 1984), adult rat ventricular myocytes (White et al., 1985), and rat lacrimal gland cells (Neyton and Trautmann, 1985).

In this paper we describe voltage dependent gating of gap junctions in salivary gland cells from *Drosophila melanogaster*. Junctional conductance is strongly dependent on both V_{i-o} and V_j and we provide the first quantitative analysis of voltage gating of this type. The data indicate that V_{i-o} and V_j dependencies reside within the same channel and that V_j dependence is influenced by V_{i-o}. Dependence on V_{i-o} and V_j may arise from a common gating domain sensitive to both potentials or from distinct, but interacting gating domains, each primarily responsive only to V_{i-o} or to V_j. Multiple gating domains may interact by virtue of their series arrangement along the channel. Some of these data have been presented in abstract form (Verselis et al., 1990).

METHODS

Preparation of cell pairs

Flies were cultured in standard cornmeal media at 25°C. Salivary glands were excised from third instar larvae and mechanically dissociated with glass microelectrodes into pairs in a solution containing (in millimolar) 100 K_2SO_4, 2 $MgSO_4$, 2 $CaCl_2$, 5 TES, 10 glucose, 0.3 mg/ml collagenase, and adjusted to pH 7.3 with KOH. The pairs are transferred to minimal *Drosophila* medium (MDM) containing (in millimolar) 36 NaCl, 34 KCl, 2 $CaCl_2$, 15 $MgCl_2$, 5 $NaHCO_3$ 10 Hepes, 2 g/L glucose, 2 g/L trehalose, and 1.8 g/L glutamine (pH 7.2 with NaOH) for electrical recording.

Measurement of junctional conductance (g_j)

Microelectrodes were pulled to resistances of 15–20 MΩ when filled with 300 mM K-citrate, 50 mM KCl, and 1 mM Hepes, pH 7.4. The electrodes were beveled to resistances of 8–10 MΩ on a rotating plate with 0.05 μm abrasive (Sutter Instrument Co., San Rafael, Ca). Each cell of a pair was impaled with two microelectrodes, one to record voltage and one to pass current. Junctional (g_j) and nonjunctional (g_{nj}) conductances were evaluated in the following manner. Each cell was clamped by an independent clamp circuit. From a common holding potential, V_h, one cell (e.g., cell 1) was stepped to a new voltage, V_1, which produced current flow, I_1, from clamp 1. Part of I_1 flowed across the nonjunctional membrane, $I_{nj(1)}$, and the rest through the junction into cell 2 as the junctional current, I_j, which was measured by clamp 2 as the current required to maintain V_2 constant. Thus, $I_j = -I_2$. Because cell 2 was maintained at V_h, g_j was directly obtained from:

$$g_j = I_j/(V_1 - V_h).$$

The nonjunctional current for cell 1 could be obtained by subtracting I_j from the total current (I_1) so that $g_{nj(1)}$ could be calculated from:

$$g_{nj(1)} = (I_1 - I_j)/(V_1 - V_h).$$

Stepping cell 2 while holding cell 1 constant allowed measurement of $g_{nj(2)}$ and provided a test for symmetry of g_j.

RESULTS

The influence of V_{i-o} on g_j

The V_{i-o} sensitivity of g_j was examined by stepping both cells of a coupled pair equally and simultaneously over a range of negative and positive membrane potentials. Equal displacement of the membrane potentials altered V_{i-o}, but maintained V_j at zero. To measure g_j small, brief hyperpolarizing voltage steps were alternately applied to each cell superimposed on the longer-duration V_{i-o} steps. The small steps did not noticeably alter g_j. Illustrated in Fig. 2 is a continuous chart record obtained from a cell pair in which V_{i-o} was examined over potentials ranging from −60 to +20 mV. Hyperpolarization from rest (−40 mV) produced little change in g_j, whereas depolarization caused g_j to decrease to a new steady state. Progressively larger depolarizations caused g_j to decrease faster and to lower steady-state values; g_j recovered to the resting value in each case upon returning the potential to −40 mV.

Steady-state g_j as a function of V_{i-o} is plotted in Fig. 3 *a* from the data in Fig. 2. The relation follows a steep sigmoid curve that asymptotically approaches a maximum at inside negative potentials and zero with increasing inside positivity. To model the steady-state data, we applied a simple reaction scheme in which channels undergo reversible transitions between open and closed states. Because gap-junction channels consist of two hemichannels, each of which may possess voltage sensitive gating elements, we considered gating by one and by two gates in series. If the channels possessed only a single gate sensitive to V_{i-o}, and the distribution between open and closed states were determined by a Boltzmann relation in which dipole moment was independent of voltage, the steady-state channel open probability, p, would be given by

$$p = 1/\{1 + \exp[A(V_{i-o} - V_o)]\}, \quad (1)$$

where V_o is the voltage at which p is 0.5 and A is a constant that expresses voltage sensitivity (Magleby and Stevens, 1972; Harris et al., 1981). If the conductance of the closed state were zero, as indicated by the near-zero junctional conductances attained at inside positive potentials, g_j would follow V_{i-o} according to

$$g_j = g_{max} p = g_{max}/\{1 + \exp[A(V_{i-o} - V_o)]\}, \quad (2)$$

where g_{max} is the maximal g_j attainable at inside negative potentials. For two identical and independent gates in series, either of which could close the channel, the probability that the channel is open would be the product of the open probabilities of the two gates. Thus, for cells at equal potentials, g_j would follow V_{i-o} according to

$$g_j = g_{max} p^2 = g_{max}/\{1 + \exp[A(V_{i-o} - V_o)]\}^2. \quad (3)$$

The appropriateness of the single and two series gate models was examined by fitting the data to the relations describing each case (Eqs. 2 and 3). The expected values of g_j and ln (g_j) are plotted in Fig. 3, *a* and *b*, respectively. Experimental data are indicated by the solid circles. For negative voltages, the relations are not distinguishable. At positive potentials the relations deviate and the data are somewhat better described by the two-series gate model. For this model, the mean value of the constant, A, was 0.085 ± .008 mV^{-1} (n = 10) which reflects an equivalent gating charge of 2.1 associated with each

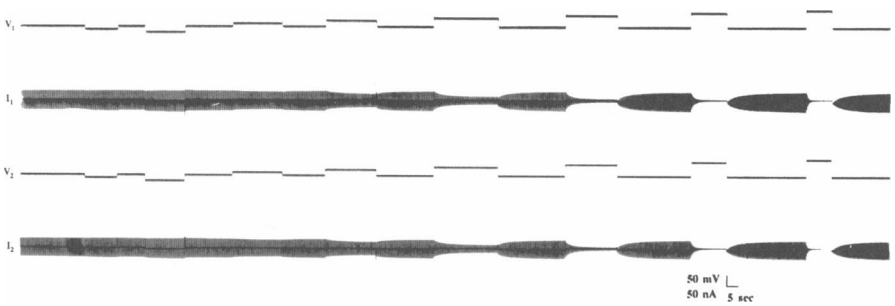

FIGURE 2 V_{i-o} dependence of g_j in salivary glands of *Drosophila melanogaster*. The four traces shown are the voltages and currents in cell 1 (*top two traces*) and cell 2 (*bottom two traces*) obtained from a cell pair in double voltage clamp. The brief upward deflections in I_1 and I_2 represent the junctional currents elicited by alternate small (10 mV), brief (100 ms) hyperpolarizing voltage steps (V_1, V_2) applied to each cell. The brief downward deflections in I_1 and I_2 represent the total currents applied to each cell in order to generate the voltage steps. g_j was obtained directly by dividing the junctional current by the voltage step. To introduce a V_{i-o}, long-duration voltage steps were applied simultaneously to both cells superimposed on the brief, alternating steps. The resting potential (V_h) for this cell pair was −40 mV at which g_j was 4.0 μS. Hyperpolarization from rest produced little change in g_j, whereas depolarization produced a reversible reduction in g_j. Successively larger depolarizations produced faster and greater reductions in g_j. Little coupling (<0.1 μS) was detectable at voltages positive to +20 mV.

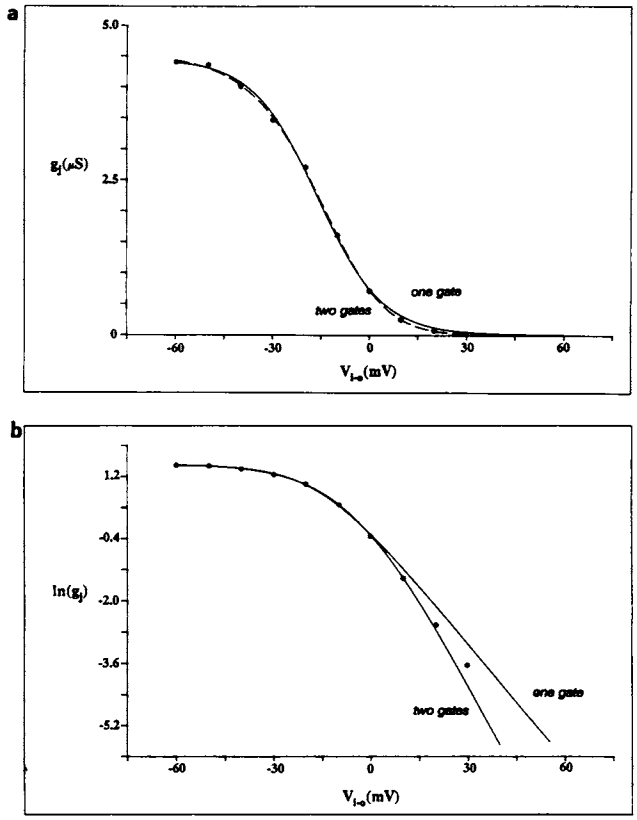

FIGURE 3 Steady-state g_j–V_{i-o} relation obtained from a single cell pair. g_j was measured over a range of holding potentials (indicated by the solid circles). The data were fit to Boltzmann relations (Eqs. 2 and 3) describing transitions between steady-state conductances for channels modeled as containing a single gate and with two independent gates in series. Fits were made by treating g_{max}, A, and V_0 as free parameters and applying a Gauss-Newton method for minimization (Jacobs, 1977). The fitted values are as follows: g_{max} = 4.4 μS, A = 0.098 mV^{-1} and V_0 = −16.1 mV for the single-gate case and g_{max} = 4.5 μS, A = 0.08 mV^{-1} and V_0 = 5.1 mV for the two gate case. (*a*) Linear plot. (*b*) Semilog plot. For either model the fit was good for $V_{i-o} < 0$. Two series gates better explains the data for $V_{i-o} > 0$.

hemichannel. Thus, the limiting slope for increasing positivity of V_{i-o} is *e*-fold per 11.5 mV in each hemichannel.

The influence of V_j on g_j

When the potential of one cell is changed relative to the other, both V_j and V_{i-o} are changed. If one assumes that there are two series gates sensitive to V_{i-o} and that V_j has no direct influence on g_j, the effects of unequal voltages of g_j between two cells can be described by two limiting cases. In one extreme, the potential sensed by each of the series V_{i-o} gates is equal to the membrane potential of the corresponding cell. The voltage sensors in this case would be located at the cytoplasmic end of the channel structure. Thus, stepping one cell would change V_{i-o} at the corresponding gate leaving V_{i-o} at the other series gate unchanged. Steady-state g_j would follow the product of the open-closed probabilities of the series gates according to

$$g_j = g_{max}/(\{1 + \exp[A(V_1 - V_o)]\}\{1 + \exp[A(V_2 - V_o)]\}). \quad (4)$$

Junctional conductance predicted from Eq. 4 is shown in Fig. 4 *a* (*dashed lines*) for the case when cell 2 is stepped over the voltage range of −75 to +75 and cell 1 is maintained at three fixed potentials (indicated on the left as V_1). The fitted curve for the g_j–V_{i-o} relation, i.e., changing V_1 and V_2 equally, is also shown (*solid line*). The curves maintain a sigmoid shape, with g_j increasing on hyperpolarization and decreasing on depolarization.

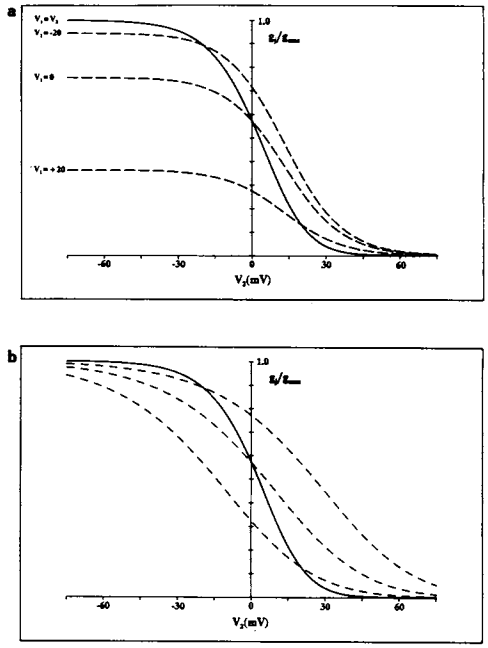

FIGURE 4 Predictions for V_{i-o} dependence with voltage steps applied to one cell. V_j is assumed to have no influence. Solid lines in *a* and *b* represent fits of V_{i-o} dependence for both cells stepped equally according to Eq. 3. (*a*) Dashed lines are theoretical g_j–V_{i-o} curves where the potential sensed by each series gate is equal to the potential in the corresponding cell (Eq. 4). One cell (V_2) is stepped between −75 and +75 mV and the other (V_1) is held at three fixed potentials, −20, 0, and +20 mV. A progressive reduction in g_{max} is evident at more positive values of V_1 as the gates on that side have a progressively lower open probability. (*b*) Theoretical g_j–V_{i-o} curves for the model that assumes the V_{i-o} sensors are at the midpoint of the channel where the potential is the mean of V_1 and V_2. The same range of V_2 and fixed values of V_1 are represented as in *a*. All the curves converge to g_{max} for hyperpolarization and zero for depolarization as the potentials sensed by the V_{i-o} gates can be made sufficiently negative or positive with large voltage steps to cell 2.

For more depolarized fixed values of V_1 there is a progressive reduction of the maximum g_j as the V_1 gates have a lower open probability. The g_j–$V_{i\text{-}o}$ curves all converge to zero with sufficient depolarization of cell 2 because all the V_2-sensitive gates would close. In each case, the dashed lines intersect the solid line where $V_1 = V_2$ and thus $V_j = 0$.

In the other extreme, the $V_{i\text{-}o}$ sensors, rather than detecting the potentials in the corresponding cells, detect the potential midway along the channel which by symmetry will be the mean of V_1 and V_2. In this case, g_j is described by

$$g_j = g_{max}/[1 + \exp(A\{[(V_1 + V_2)/2] - V_o\})]^2. \quad (5)$$

Thus, the relation for a change in the potential of one cell would be the same as that for equal changes in both cells except that the apparent voltage sensitivity would be reduced by half and the effective V_o would be shifted. The g_j–$V_{i\text{-}o}$ curves according to Eq. 5 are shown in Fig. 4 *b* for the same values of V_1 and V_2 as in Fig. 4 *a*. In each case g_j converges to g_{max} at inside negative values of V_2 because sufficient hyperpolarization of cell 2 would bring $V_{i\text{-}o}$ midway along the channel into the plateau region of the g_j–$V_{i\text{-}o}$ curve. As in the first limiting case, convergence to zero occurs when one cell is made sufficiently inside positive.

Neither Eqs. 4 or 5 adequately described the effects of unequal voltages in cell pairs. Fig. 5 *a* shows a series of depolarizing and hyperpolarizing steps applied to cell 2 from a holding potential of −20 mV (*top*) and the elicited junctional currents, I_j (*below*). Rather than increasing with hyperpolarization and decreasing with depolarization as for $V_{i\text{-}o}$, g_j decreased with both polarities of V_2 as evidenced by the decay in I_j to a lower value from an initial peak. For either polarity, I_j decayed more rapidly and reached a lower steady-state value as the magnitude of the V_2 step was increased. Depolarization of cell 2 caused a faster and larger decrease in I_j than the same degree of hyperpolarization. Essentially equal changes in amplitude and time course of junctional currents were seen when V_1 was stepped and V_2 was held constant (data not shown). Steady-state g_j as a function of V_2 is plotted in Fig. 5, *b* and *c*, for fixed V_1 values of −20 and 0 mV, respectively. The solid lines are fits to the data for g_j when both V_1 and V_2 were stepped equally (points not shown). The dashed lines are the curves predicted from Eqs. 4 and 5. Experimental data for steps to cell 2 (*squares*) deviated markedly from the prediction of either model. Most dramatically, g_j was reduced by hyperpolarization when only an increase was predicted. For moderate depolarization (e.g., stepping cell 2 to 0 and +10 mV from a fixed potential of −20 mV, Fig. 5 *b*), the reduction in g_j was greater than for the same depolarization applied to both cells. For larger depolarizations from −20 mV (Fig. 5 *b*) or smaller steps from 0 mV (Fig. 5 *c*), the degree of reduction in g_j was less than for equal depolarization of both cells, but remained greater than predicted by Eqs. 4 or 5 which assume $V_{i\text{-}o}$ to be the only determinant of g_j. These results can be explained by the coexistence of two voltage sensitivities: a V_j sensitivity that reduces g_j for both polarities of V_j and a $V_{i\text{-}o}$ sensitivity that increases g_j on hyperpolarization and reduces it on depolarization. The effectiveness of hyperpolarizing one cell in reducing g_j requires that there be V_j sensitivity, which is confirmed by the greater than predicted reduction in g_j by moderate depolarization of one cell. By virtue of the polarity dependent influence of $V_{i\text{-}o}$, the decrease in g_j is asymmetric around $V_j = 0$ with depolarization causing a larger decrease in g_j than comparable hyperpolarization. The minimum g_j's for large hyperpolarizations and depolarizations of one cell were not determined because of the large nonjunctional membrane currents required. For inside positivities of one cell >40 mV g_j appeared to remain greater than zero suggesting there may be a residual (minimum) g_j. The existence of a residual g_j would require that closure by V_j were incomplete and that large depolarizations of one cell prevented complete closure by the $V_{i\text{-}o}$ gating mechanism, i.e., the actions of $V_{i\text{-}o}$ and V_j were interdependent. Evidence for interaction between V_j and $V_{i\text{-}o}$ gating mechanisms is presented below.

Time course of changes in g_j with step changes in $V_{i\text{-}o}$

The time course of the decrease in g_j for $V_{i\text{-}o}$ steps (equal changes in V_1 and V_2) was measured with small, brief hyperpolarizing voltage steps as in Fig. 2. In the example in Fig. 6 *a*, the initial holding potential was −40 mV and the cells were stepped to potentials of +10, +20, and +30 mV. For channels with first order reversible transitions between open and closed states, the open probability would reach a new steady state according to

$$p = p_\infty + (p_o - p_\infty)\exp(-t/\tau), \quad (6)$$

where τ is the time constant and p_o and p_∞ are the initial and equilibrium values for the open probabilities. For two series gates and equal $V_{i\text{-}o}$'s in the two cells, the initial and equilibrium open probabilities of the individual gates (p_o and p_∞) could be measured as $p_o = \sqrt{(g_o/g_{max})}$ and $p_\infty = \sqrt{(g_\infty/g_{max})}$. Because the fraction of channels

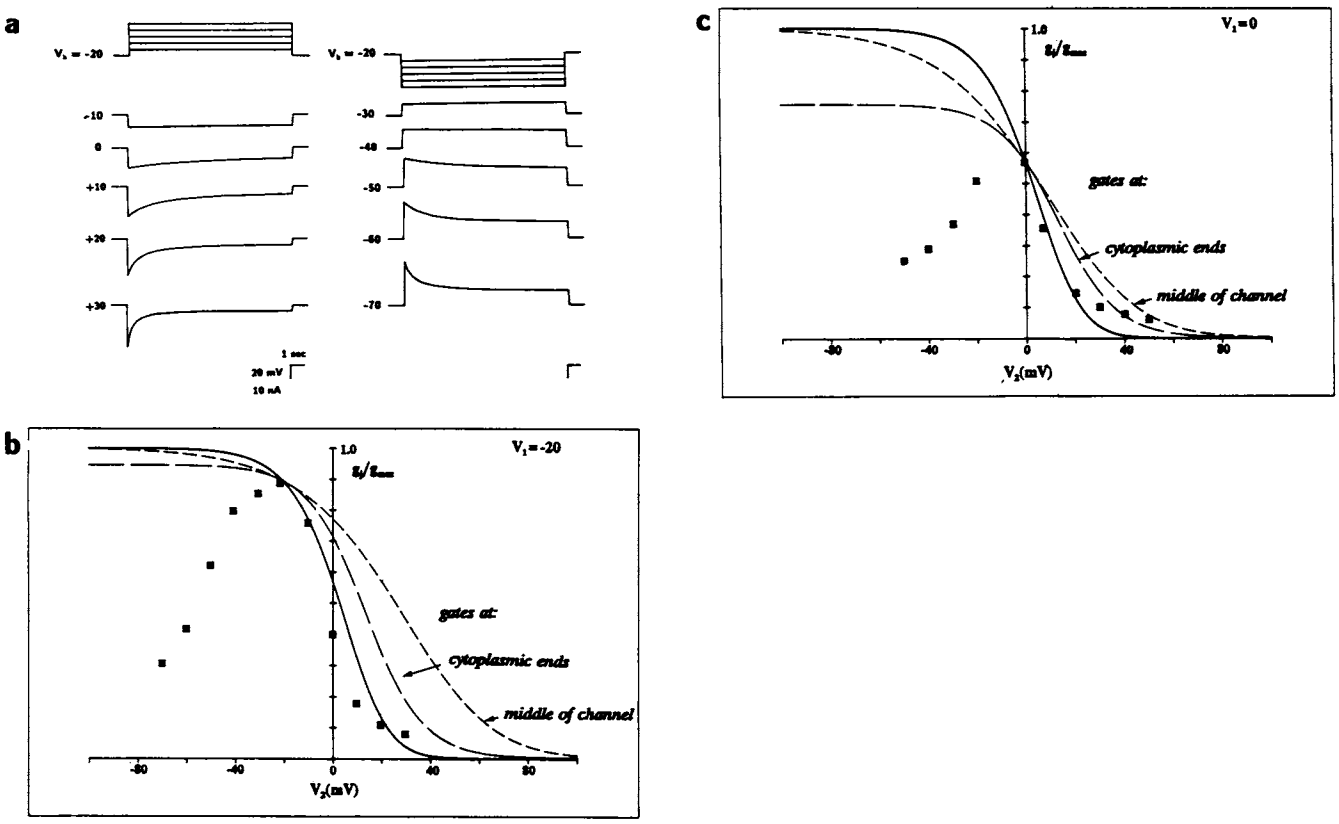

FIGURE 5 Effects of transjunctional voltage on g_j. (*a*) A series of current and voltage records for depolarizing (*left traces*) and hyperpolarizing (*right traces*) voltage steps applied to cell 2. Holding potential for this cell pair was −20 mV (indicated as V_h). Voltage steps are superimposed above and the junctional currents (I_j) are below; numbers on the left indicate the applied potential. For either polarity, successively larger voltage steps produced larger initial I_j's which decayed faster and to a greater degree. For hyperpolarization the decay in I_j was less and slower than for comparable depolarization. g_j, obtained by dividing I_j by the voltage step, was normalized to g_{max}. g_{max} was obtained as described in Fig. 3, *b* and *c*. Steady-state g_j normalized with respect to g_{max} was plotted as a function of voltage in the stepped cell. The solid line in each plot is a fit to the data obtained by stepping both cells equally (same data and cell pair as Fig. 3, data points not shown). The dashed lines represent the steady-state g_j–$V_{i\text{-}o}$ curves for steps to one cell predicted by the models with $V_{i\text{-}o}$ sensors at the cytoplasmic end of the channel and in the middle of the channel (as indicated). The cells were held at −20 mV for *b* and 0 mV for *c*. Data points (*solid squares*) deviate markedly from predictions of either model. Hyperpolarization caused a reduction (rather than an increase) in g_j, and the reduction in g_j on depolarization was greater than predicted for either depolarizing both cells equally or depolarizing only one cell. These data demonstrate V_j sensitivity that reduced g_j for both polarities of V_j.

open would be determined by the product of the open probabilities of the series gates, g_j would be described by

$$g_j = g_{max}p^2 = [\sqrt{g_\infty} + (\sqrt{g_o} - \sqrt{g_\infty})\exp(-t/\tau)]^2. \quad (7)$$

Thus, plotting $\ln\{(\sqrt{g_j} - \sqrt{g_\infty})/(\sqrt{g_o} - \sqrt{g_\infty})\}$ vs time for a channel with two series gates would produce a linear relation with a slope equal to the rate constant $(1/\tau)$ describing transitions between steady-state open probabilities for each hemichannel. Fig. 6 *b* shows these plots for the data in Fig. 6 *a*. The solid lines represent fits to the data with g_∞, g_o, and τ treated as free paramaters. The fits were good for all three $V_{i\text{-}o}$ steps indicating that the model of two series gates that follow first order kinetics adequately predicts the relaxation in g_j when the voltages in the cells are displaced equally. The calculated time constants for changes in open probability of each gate were generally slow, with values of 3.3, 1.9, and 1.3 s for the $V_{i\text{-}o}$ steps to +10, +20, and +30 mV shown in Fig. 6 *a*. The model depicting a single gate also provided a good fit to the data (not shown) so that analysis of these kinetic data do not provide a sufficiently sensitive test to distinguish between the one and two gate models. In the one gate model the calculated time constants would be somewhat shorter.

Exponential relaxations for the series gates can be described in terms of forward, α, and reverse, β, rate constants (see Magleby and Stevens, 1972; Harris et al., 1981). The rate constants for $V_{i\text{-}o}$ dependence can be

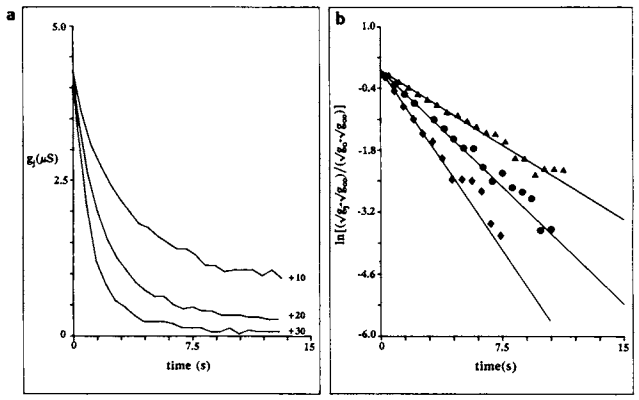

FIGURE 6 Time course of the decrease in g_j for $V_{i\text{-}o}$ steps to +10, +20, and +30 mV from a holding potential of −40 mV. g_j was measured with small, brief hyperpolarizing steps applied to one cell superimposed on the $V_{i\text{-}o}$ steps as in Fig. 2. The decline in g_j was faster for more positive voltages. (*a*) Linear plot. (*b*) Plot according to Eq. 7 to show single exponential behavior according to the series gate model. A least squares method was used to obtain linear fits (*solid lines*) to the data (*solid symbols*). Fits for each voltage step were good (correlation coefficients >0.99). Time constants for the three $V_{i\text{-}o}$ steps to +10, +20, and +30 mV were 3.3, 1.9, and 1.3 s, respectively.

calculated from the time constants and steady-state open probabilities with equal voltage steps to both cells. For a Boltzmann process, rate constants depend on voltage according to equations of the form (see Harris et al., 1981)

$$\alpha = \lambda \exp [A_\alpha(V_{i\text{-}o} - V_o)]$$
$$\beta = \lambda \exp [A_\beta(V_{i\text{-}o} - V_o)], \quad (8)$$

where A_α and A_β are the voltage sensitivities of the opening and closing rate constants, respectively, and λ is the rate constant at which $V_{i\text{-}o} = V_o$ and $\alpha = \beta$. We calculated α and β from $\alpha = p_\infty/\tau$ and $\beta = (1 - p_\infty)/\tau$ using Eq. 3 to obtain g_{max} and Eq. 7 to obtain g_∞ and τ for several different $V_{i\text{-}o}$ steps. Calculations were made from the decay in g_j for a series of depolarizing steps to both cells starting at −40 mV and from the recovery in g_j upon returning to −40 mV. Time constants at any given $V_{i\text{-}o}$ were independent of the previous value of $V_{i\text{-}o}$ as determined by rates of recovery from a series of inside positive potentials and from reductions in g_j after a series of inside negative potentials (data not shown). The exponential relations describing α and β are plotted in Fig. 7 *a*. The data from this cell pair were best fit with the expressions

$$\alpha = 0.168 \exp [-0.017(V_{i\text{-}o} - 7.7)]$$
$$\beta = 0.168 \exp [0.064(V_{i\text{-}o} - 7.7)] \quad (9)$$

The predicted dependence of the calculated time constant on $V_{i\text{-}o}$ is illustrated in Fig. 7 *b*. The curve was obtained from $\tau = 1/(\alpha + \beta)$, with α and β determined from the expressions in Eq. 9. The time constants for equal steps to both cells ranged from several seconds at moderate inside negative potentials to several hundred milliseconds at inside positive potentials >40 mV. The faster time constants at inside positive potentials reflect the steep voltage dependence of the rate constant for closing, which is approximately fourfold more sensitive to voltage than the opening rate.

Time course of changes in g_j caused by step changes in V_j

Voltage steps applied to one cell induced changes in g_j that were more complex than the simple decay exhibited during equal steps to both cells. Kinetic and steady-state changes in g_j depended not only on the amplitude and polarity of the voltage step applied to one cell, but also on the holding potential from which the step was applied. Fig. 8 shows junctional currents, I_j elicited by ±30 and ±50 mV steps applied to one cell of a pair. The I_j's for each represented voltage step were elicited from three different holding potentials (−40, −20, and 0 mV) and were normalized to their respective peaks and superimposed to illustrate their relative time courses. For large negative steps (e.g., −50 mV) from the most positive holding potential shown (0 mV), the time course in I_j consisted of a fast decrease followed by a slow increase (Fig. 8 *b*). For large positive steps from a negative holding potential (e.g., −40 mV), an initial rapid decrease was followed by a continued, but slower decrease (Fig. 8 *d*). These complex waveforms can be explained by invoking both V_j and $V_{i\text{-}o}$ dependent mechanisms. The initial decrease in I_j for both voltage polarities is ascribable to channel closing by V_j. The subsequent slower increase or decrease in I_j is ascribable to channel opening and closing for hyperpolarizing and depolarizing $V_{i\text{-}o}$'s, respectively. $V_{i\text{-}o}$ would be expected to contribute little upon hyperpolarization from the negative plateau region of the g_j–$V_{i\text{-}o}$ curve, which explains the absence of the slow increase in I_j for large hyperpolarizing steps applied from negative holding potentials (e.g., $V_{i\text{-}o} = -40$ mV).

V_j reduced g_j faster and more effectively at more positive $V_{i\text{-}o}$'s. Thus, for either polarity, the initial decay in I_j was faster as the holding potential was made more positive (compare traces within each panel of Fig. 8). Also, the initial decay in I_j for positive steps at any holding potential (Fig. 8, *c* and *d*) was consistently faster than for comparable steps in the hyperpolarizing direction (Fig. 8, *a* and *b*). The steady-state changes in g_j produced by stepping one cell also depended on $V_{i\text{-}o}$. For hyperpolarizing steps applied to one cell, the fractional reduction in I_j decreased with larger steps ascribable to

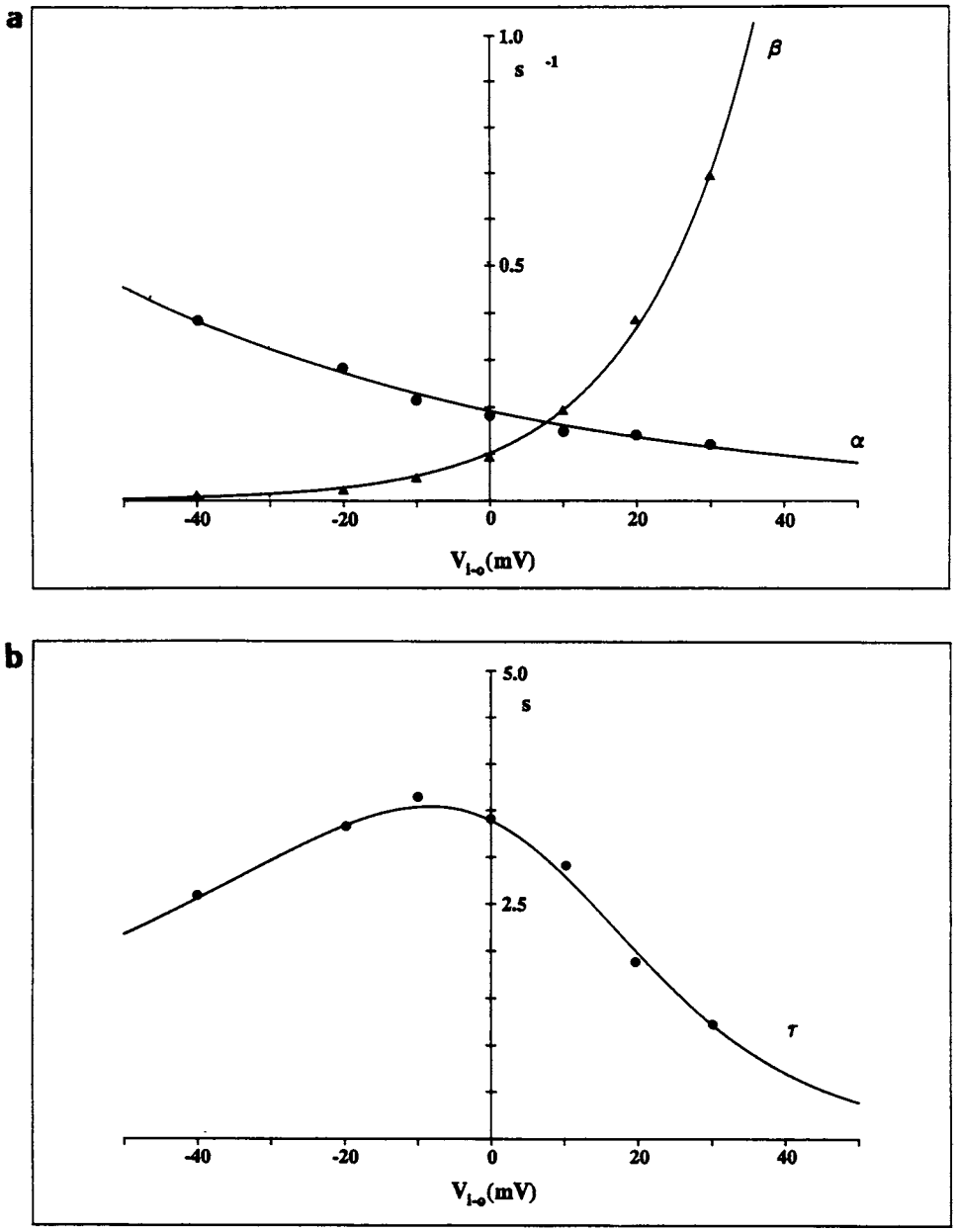

FIGURE 7 $V_{i\text{-}o}$ dependence of kinetic parameters. (*a*) Rate constants for opening (α) and closing (β) by $V_{i\text{-}o}$. α and β were calculated from $\alpha = p_\infty/\tau$ and $\beta = (1 - p_\infty/\tau$ where p_∞ is the steady-state open probability and τ is the time constant of relaxation of open probability from Eq. 7. These values of α and β (*solid symbols*) are plotted as a funciton of $V_{i\text{-}o}$. The smooth curves are exponentials according to Eq. 8 obtained by a least squares fit to the semilog plot (not shown). Voltage sensitivity of β is fourfold greater than that for α. (*b*) $V_{i\text{-}o}$ dependence of the time constants for transition between open probabilities. The smooth curve was obtained from $1/(\alpha + \beta)$ with α and β representing expected values obtained from exponential fits to the data described in *a*. The time constant for $V_{i\text{-}o}$ displayed a maximum at −10 mV of ~3.55 and declined steeply at positive potentials.

the action of more negative $V_{i\text{-}o}$ to increase g_j. For depolarizing steps of moderate size, e.g., +30 mV, steady-state I_j relative to the peak decreased slightly with increasing positivity of the holding potential, whereas for larger steps, e.g., +50 mV, the relative decrease from the peak remained constant suggesting that the fractional reduction in g_j by V_j had reached its maximum degree.

The initial reductions in g_j attributed primarily to V_j were faster than the changes caused by $V_{i\text{-}o}$ and should provide estimates of time constants for V_j dependence. Because both hyperpolarizing and depolarizing steps

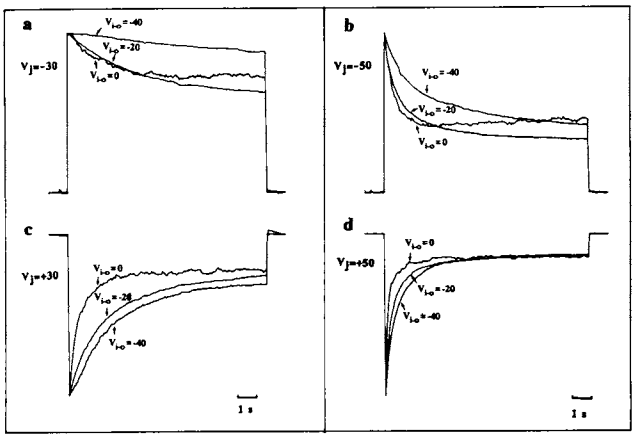

FIGURE 8 Time course of V_j dependence and effect of V_{i-o}. Junctional currents illustrating the time course of the changes in g_j elicited by ±30 (*a* and *c*) and ±50 (*b* and *d*) mV steps to one cell. The steps were applied from three V_{i-o} potentials; −40, −20, and 0 mV (as indicated). I_j's were each normalized to their initial values upon generating V_j and superimposed to illustrate the relative rates of decay. For hyperpolarizing steps of −30 or −50 mV (*a* and *b*) g_j decreased faster and to proportionately lower steady-state values as V_{i-o} was changed from −40 to −20 mV. At a V_{i-o} of 0 mV the initial decrease was faster still, but steady-state g_j increased ascribable to the influence of a hyperpolarizing V_{i-o}. For depolarizing steps of +30 mV (*c*), g_j decreased faster and apparently to slightly lower steady-state values as V_{i-o} was made more positive. For the larger +50 mV depolarizing steps (*d*), the decay was faster with more positive V_{i-o}'s, but the fractional decrease in g_j remained constant suggesting that V_j's effect had reached a maximum.

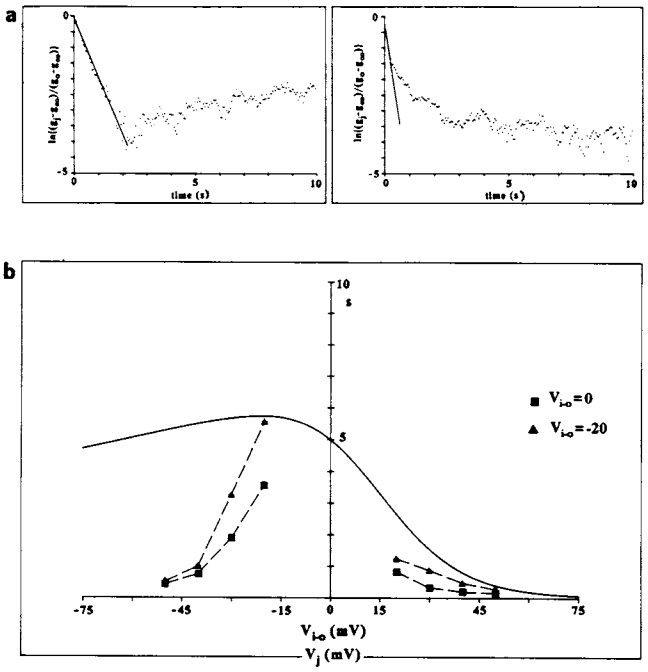

FIGURE 9 Comparison of time constants of V_j and V_{i-o} dependence. (*a*) Examples of the initial decay in g_j for V_j steps. Shown are −50 mV (*left*) and +50 mV (*right*) steps to one cell from a holding potential of 0 mV. Data are plotted as $\ln [(g_j - g_\infty)/(g_o - g_\infty)]$ vs time. g_∞ was chosen as the minimum value reached during the applied pulse. The straight lines represent linear fits to the initial decrease in g_j. (*b*) The smooth curve represents the voltage dependence of the time constant for V_{i-o} dependence of open probability fitted from data (not shown) for this cell pair. The symbols connected by lines are measured time constants for V_j obtained by extracting the fast component of the change in g_j for voltage steps applied to one cell. Data for V_j are shown from holding potentials of 0 mV (■) and −20 mV (▲). All data for V_j and V_{i-o} were obtained from the same cell pair. Time constants were faster for depolarizing V_j's than for comparable hyperpolarizing V_j's. Time constants for V_j were faster for either polarity with increasing positivity of V_{i-o}.

applied to one cell reduce g_j and because of symmetry, it is likely that there is a V_j gate in each of the apposed membranes (Harris et al., 1981). In this model, a V_j step of one polarity would close one gate and maintain the other open; the configuration is reversed for the other polarity of V_j. For closure of a single gate that exhibits first order kinetics, a plot of $\ln [(g_j - g_\infty)/(g_o - g_\infty)]$ vs time produces a straight line with a slope equal to the rate constant for transitions between steady states. Representative fits applied to the early phase of the decrease in g_j are shown in Fig. 9 *a* for ±50 mV steps applied from a holding potential of 0 mV. The appropriate value to choose for g_∞ depends somewhat on the model for V_{i-o} and V_j interactions, but the time constant should be insensitive to g_∞ (see Fig. 9 *a* legend). The initial rate was faster for depolarization (τ = 0.19 s, *right*) than for hyperpolarization (τ = 0.45 s, *left*). Data for several V_j steps applied from two holding potentials (−20 and 0 mV) and for equal steps to both cells are plotted in Fig. 9 *b* with the curve of τ for V_{i-o}. Over most of the voltage range, V_j acted considerably faster than V_{i-o} to change g_j. The V_j component was faster for more depolarized holding potentials and it was faster for depolarizing than for hyperpolarizing steps at a given holding potential.

DISCUSSION

We demonstrated here that in larval salivary gland cells of *Drosophila melanogaster* g_j is markedly affected by two kinds of voltage differences that we have termed V_{i-o} and V_j. The gap-junction channel is composed of two halves joined in the extracellular gap between two closely apposed cells and there is evidence that the lumen of the channel is insulated from the extracellular gap and that the gap is freely accessible to the bathing medium (Bennett, 1977). Thus, V_{i-o} is established between the

cytoplasm and the exterior of the cells (see Fig. 1). In the case of two cells placed at the same potential, $V_{i\text{-}o}$ would be uniform across the channel wall in the region of the gap. With cells at unequal potentials, i.e. when V_j is present, a voltage gradient is established along the lumen of the channel that also modifies the potential across the channel wall, although nonuniformly along its length. Thus, changing the potential equally in both cells establishes a uniform $V_{i\text{-}o}$, whereas changing the potential of one cell establishes both $V_{i\text{-}o}$ and V_j differences, with $V_{i\text{-}o}$ nonuniform along the lumen of the channel.

Changes in g_j brought about by $V_{i\text{-}o}$ and V_j differ in kinetics and sensitivity to voltage suggesting that $V_{i\text{-}o}$ and V_j act upon different gating mechanisms. For $V_{i\text{-}o}$ dependence, steady-state data are somewhat better fit by a model with two independent $V_{i\text{-}o}$ gating domains arranged in series. The serial arrangement of the gating domains is a likely consequence of the serial arrangement of the two hemichannels, each of which possesses a separate gating domain. A similar series gate arrangement was used to model V_j dependence in amphibian blastomeres (Harris et al., 1981) and $V_{i\text{-}o}$ dependence in *Chironomus* salivary glands (Obaid et al., 1983). Recent data on formation of heterotypic junctions between *Xenopus* oocytes expressing different connexins support the hypothesis of separate gates (Swenson et al., 1989; Barrio et al., 1990). Our kinetic data did not allow distinction between single and two series gate models. Although we favor the view that two separate $V_{i\text{-}o}$ gates are present in the *Drosophila* salivary gland channels, our data do not exclude the possibility of a single $V_{i\text{-}o}$ gating domain. Because of symmetry, a single $V_{i\text{-}o}$ gating domain would be most plausible as formed at the junction of the two hemichannels in the intercellular gap region of the channel.

The sensitivity of $V_{i\text{-}o}$ dependence in *Drosophila* salivary glands is comparable to that for voltage-gated ion channels in excitable membranes, although the changes in conductance are considerably slower (see Hille, 1984). For a two series $V_{i\text{-}o}$ gate model, the value of the constant, A, is a measure of the voltage sensitivity for each hemichannel. The value of $0.085 \pm .008$ mV^{-1} in *Drosophila* salivary glands represents an equivalent elementary gating charge of ~2. Thus, the open probability of each hemichannel has a limiting slope of e-fold per 11.5 mV in this tissue. This value is similar to that for $V_{i\text{-}o}$ in *Chironomus* salivary glands (Obaid et al., 1983). V_j dependence in amphibian blastomeres is somewhat steeper, displaying an equivalent gating charge of 6 and a limiting slope of e-fold changes in g_j occurring every 4–5 mV (Spray et al., 1981). For small depolarizations Na^+ and K^+ channels increase their conductance with a slope of e-fold for every 4.0 and 5.5 mV, respectively (see Hille, 1984).

The time constants for $V_{i\text{-}o}$ dependence in *Drosophila* salivary glands vary considerably, being <1 s for voltage steps to potentials more positive than +40 mV and 4–5 s at moderately negative potentials. The reduction in g_j appears to result predominantly from a steep voltage dependence of closing which is fourfold more sensitive than the opening rate (Fig. 7). The V_j dependent changes are faster than the $V_{i\text{-}o}$ dependent changes over a large voltage range (Fig. 9). In amphibian blastomeres time constants of relaxation of g_j are 0.2 s for V_j steps of ±20 mV (Harris et al., 1981). Analysis of V_j dependence in *Drosophila* is complicated by the presence of $V_{i\text{-}o}$ dependence, as well as by the influence of $V_{i\text{-}o}$ on V_j dependence. At negative $V_{i\text{-}o}$'s within the plateau of the g_j–$V_{i\text{-}o}$ relation, reductions in g_j by hyperpolarizing steps to one cell can be predominantly attributed to V_j. In this region, V_j dependence was relatively weak and somewhat slow compared to that in amphibian blastomeres. For a V_j of 50 mV generated by hyperpolarization of one cell, time constants were 0.8–1.0 s and g_j remained at 30–40% of the maximum. Both the speed and the degree of reduction of g_j increase at more positive holding potentials. At $V_{i\text{-}o}$'s more positive than +20 mV, time constants for large V_j's resemble those measured in amphibian blastomeres.

$V_{i\text{-}o}$ and V_j dependencies reside in the same channel and interact

Dependence on $V_{i\text{-}o}$ and V_j in *Drosophila* clearly resides in the same channel and not two distinct populations of channels, one sensitive to V_j and the other to $V_{i\text{-}o}$. This is evident from the almost complete block of g_j caused by large positive $V_{i\text{-}o}$'s and the substantial reduction in g_j caused by hyperpolarizations to one cell. However, even large V_j's did not reduce g_j to near zero. Although very large V_j's could not be applied without damaging the cell, the g_j–V_j relation sometimes appeared to asymptote the at a nonzero g_j. All V_j dependent junctions examined thus far exhibit a voltage insensitive (residual) g_j comprising between 5 and 50% of the maximum g_j at $V_j = 0$ (see Spray et al., 1985). A residual g_j may in part be an artifact of the inability to apply large enough voltages. Other possibilities include a lack of V_j sensitivity in some channels, a nonzero minimum channel open probability or a nonzero minimum conductance state (i.e., partial closure). In *Drosophila*, if $V_{i\text{-}o}$ and V_j acted independently, g_j would be reduced to zero with a sufficiently large depolarization applied to one cell because voltage steps applied to one cell would have a $V_{i\text{-}o}$ component in addition to a V_j component, which if sufficiently positive, would close the channels; the g_j–$V_{i\text{-}o}$ relation converges

to zero with positivity (Fig. 4). Thus, the persistence of a residual g_j at very large V_j's would require that V_{i-o} and V_j gating mechanisms interact in some manner. Similarly, the effect of V_{i-o} on the time constants of V_j induced changes in g_j require some form of interaction. Although the existence of channels lacking V_j gates cannot be ruled out by our data, a lack of V_j gates cannot explain a residual g_j because channels lacking V_j gates would close due to V_{i-o} dependence and would not, therefore, contribute to a residual g_j. Similar arguments can be made against V_j gating with a nonzero minimum conductance or a nonzero channel open probability. In the V_j-sensitive amphibian blastomeres, where g_j is unaffected by V_{i-o}, proportional reductions in g_j and in junctional permeability to large ions upon application of V_j suggest that voltage closes gap-junction channels in an all-or-none rather than a graded manner (Verselis et al., 1986). Although the existence of substates that do not change relative permeabilities cannot be ruled out by these data, they are suggestive of a mechanism in which gating by V_j converges to a minimum nonzero channel open probability. Single-channel studies are ultimately necessary to resolve these issues.

Possibilities for interactions between V_{i-o} and V_j

Do V_j and V_{i-o} sensitivities result from the actions of separate domains in the channel protein or is there a single domain capable of responding to both applied potentials? The influence of V_{i-o} on V_j sensitivity does not preclude the existence of separate domains, but simply indicates that V_{i-o} affects the V_j domain. A model of channel closure by tilting of the subunits, as proposed by Unwin (1989), would suggest a unitary mechanism. However, the markedly different kinetics of V_j and V_{i-o} closure suggest that the closed states associated with each of these mechanisms are different. Because gap-junction channels are formed by two apposed hemichannels, separate domains for gating by V_{i-o} and V_j would require that each channel possess four distinct gating structures, two per hemichannel. An interesting possibility for interactions among multiple gating structures within a single channel exists in the form of contingent gating whereby the local field within the channel is affected by the state of each of the series gates (Harris et al., 1981). Each of the gates and/or sensors react independently to the local field, but closure of the channel by one gate can change the electric field detected by the other gate(s) and/or sensor element(s). In this model, V_{i-o} and V_j gating domains do not interact directly and the response of each gating domain to voltage remains unchanged.

If the V_{i-o} and V_j gating domains are separate and in series, changes in the local electric field at each of the series gates would depend on where the gates were situated relative to one another. Given that two cells placed at the same potential establish this same potential between the lumen of the channel and the extracellular gap, it is possible that V_{i-o} gates are situated in the part of the channel wall that spans the intercellular gap. Thus, a possible configuration of four separate gates would have V_{i-o} gates deep in the channel, near the juncture of the hemichannels, and the V_j gates closer to the cytoplasmic entrances to the channel. In this configuration, depolarization of one cell would elicit channel closure by V_j or V_{i-o}. Because the kinetics of V_j closure are substantially faster than V_{i-o} over a wide range of voltages, the most predominant form of channel closure would be by V_j. If V_j closed the V_j gate on the relatively positive side of the channel (Verselis et al., 1987; Bennett et al., 1988; Swenson et al., 1989), the local field would collapse around the closed V_j gate (corresponding to the stepped cell) leaving the potential at the inner V_{i-o} gates relatively unchanged. Conversely, hyperpolarization of one cell would tend to close the V_j gate in the unstepped cell and would bring the V_{i-o} gates to the newly stepped potential. For hyperpolarization or depolarization of one cell, stochastic opening and closing of the V_j gate would subsequently change the potential at the V_{i-o} gates and alter their open probabilities accordingly, which would, in turn, affect the V_j gate. The resulting steady-state condition for series gates could involve cycling between states representing combinations of open and closed V_j and V_{i-o} gates in both hemichannels. A cycling scheme involving two gates was proposed to explain voltage gating in squid blastomeres (Bennett and Spray, 1984).

Another possibility for contingent gating exists in the form of allosteric interactions between gating domains. Changes in the conformation of one gating domain could alter the conformation of another gating domain and affect its response to voltage.

Although the four-series gate model is conceivable, we cannot rule out the possibility that the channels contain only two series gates, one per hemichannel, with each gate sensitive to both V_j and V_{i-o}. In such a case, changes in g_j would be expected to behave in a complex manner dependent on the resultant electric field the sensors experience.

The possibility of dual voltage control is a unique property of gap-junction channels. Gating of g_j by voltage provides a rapid and reversible means of altering communication between cells and is an attractive mechanism for a number of physiological processes. In embryonic tissues, voltage dependence could be used to control cell–cell interactions involved in regional specification during primary induction. The dynamics of V_j

dependent coupling in embryonic cells was analyzed by modeling in Harris et al. (1983). In neurons, voltage dependent junctions offer a mechanism of synaptic control. For V_{i-o} dependence in particular, control of intercellular communication may be linked to changes occurring at the plasma membrane as activation or inhibition of ion channels can lead to changes in the membrane potential that, in turn, alter junctional coupling. Secretory cells, such as in the mammalian salivary gland, contain voltage- and ligand-gated channels which appear to play a role in the process of secretion and ion transport (Peterson, 1987). It has been postulated that intercellular coupling in secretory epithelia maintains uniform membrane potentials that are essential for transport function (Peterson, 1985). Further mechanistic descriptions of gap-junction gating by voltage together with molecular analyses should provide insight as to the nature of V_{i-o}- and V_j-dependent gating.

We are indebted to R. L. White for the design and construction of the high-voltage dual voltage clamp. We also thank H. L. Harris for helpful comments on the manuscript.

This work was supported by National Institutes of Health grants HD-04248 and NS-07512. M. V. L. Bennett is the Sylvia and Robert S. Olnick Professor of Neurosciences.

Received for publication 31 July 1989 and in final form 3 August 1990.

REFERENCES

Auerbach, A. A., and M. V. L. Bennett. 1969. A rectifying electrotonic synapse in the central nervous system of a vertebrate. *J. Gen. Physiol.* 53:211–237.

Barrio, L. C., T. Suchyna, T. Bargiello, R. Roginski, R. S. Zukin, B. Nicholson, and M. V. L. Bennett. 1990. Voltage dependence and rectification at rat connexin 26 and 32 junctions expressed in *Xenopus* oocytes. *Abstr. Soc. Neurosci.* 16: 185.

Bennett, M. V. L. 1977. Electrical transmission: a functional analysis and comparison with chemical transmission. *In* Cellular Biology of Neurons. Handbook of Physiology. The nervous System. Vol. 1. E. R. Kandel, editors. Williams and Wilkins, Baltimore, MD. 357–416.

Bennett, M. V. L., and D. C. Spray. 1984. Gap junctions: two voltage dependent gates in series allow voltage induced steady-state cycling around a circular reaction scheme. *Biophys. J.* 45:60a. (Abstr.)

Bennett, M. V. L., V. K. Verselis, R. L. White, and D. C. Spray. 1988. Gap junctional conductance: gating. *In* Gap Junctions. E. L. Hertzberg and R. Johnson, editors. Alan R. Liss, New York.

Beyer, E. C., D. L. Paul, and D. A. Goodenough. 1987. Connexin 43: a protein from rat heart homologous to a gap junction protein from liver. *J. Cell. Biol.* 105:2621–2629.

Caterall, W. A. 1988. Structure and function of voltage-sensitive ion channels. *Science* (*Wash. DC*). 242:50–61.

Ebihara, L., E. C. Beyer, K. I. Swenson, D. A. Paul, and D. A. Goodenough. 1989. Cloning and expression of a *Xenopus* embryonic gap junction protein. *Science* (*Wash. DC*). 243:1194–1195.

Furshpan, E. J., and D. D. Potter. 1959. Transmission at the giant motor synapses of crayfish. *J. Physiol.* (*Lond.*). 145:289–325.

Giaume, C., and H. Korn. 1985. Junctional voltage dependence at the crayfish rectifying synapse. *In* Gap Junctions. M. V. L. Bennett and D. C. Spray, editors. Cold Spring Harbor Laboratory, Cold Spring Harbor, NY. 367–379.

Gimlich, R. L., N. M. Kumar, and N. B. Gilula. 1988. Sequence and developmental expression of mRNA coding for a gap junction protein in *Xenopus*. *J. Cell Biol.* 107:1065–1073.

Harris, A., D. C. Spray, and M. V. L. Bennett. 1981. Kinetic properties of a voltage-dependent junctional conductance. *J. Gen. Physiol.* 77:95–117.

Harris, A. L., D. C. Spray, and M. V. L. Bennett. (1983). Control of intercellular communication by voltage dependent gap junctional conductance. *J. Neurosci.* 3:79–100.

Hille, B. 1984. Ion Channels of Excitable Membranes. Sinauer Associates Inc., Sunderland, MA. 426 pp.

Jacobs, D. A., editor. 1977. The State of the Art in Numerical Analysis. Academic Press, Inc., NY.

Jaslove, S., and P. R. Brink. 1986. Mechanism of rectification at the electrotonic motor giant synapse of the crayfish. *Nature* (*Lond.*). 323:63–65.

Johnston, M. F., and F. Ramon. 1982. Voltage independence of an electrotonic synapse. *Biophys. J.* 39:115–117.

Knier, J., and M. V. L. Bennett. 1985. Voltage dependence of gap junctions in tunicate embryos. *Biol. Bull.* 169:3. (Abstr.)

Kumar, N. M., and N. B. Gilula. 1986. Cloning and characterization of human and rat liver cDNAs coding for a gap junction protein. *J. Cell Biol.* 103:767–776.

Magleby, K. L., and C. F. Stevens. 1972. The effect of voltage on the time course of endplate currents. *J. Physiol.* (*Lond.*). 223:151–171.

Makowski, L., D. L. D. Casper, W. C. Phillips, and D. A. Goodenough. 1977. Gap junction structures. II. Analysis of x-ray diffraction data. *J. Cell Biol.* 74:629–645.

Margiotta, J. F., and B. Walcott. 1983. Conductance and dye permeability of a rectifying electrical synapse. *Nature* (*Lond.*). 305:52–55.

Neyton, J., and A. Trautmann. 1985. Single channel currents of an intercellular junction. *Nature* (*Lond.*). 317:331–335.

Obaid, A. L., S. J. Socolar, and B. Rose. 1983. Cell-to-cell channels with two independently regulated gates in series; analysis of junctional conductance by membrane potential, calcium and pH. *J. Membr. Biol.* 73:69–89.

Paul, D. L. 1986. Molecular cloning of cDNA for rat liver gap junction protein. *J. Cell Biol.* 103:123–134.

Peterson, O. 1985. Importance of electrical cell-cell communication in secretory epithelia. *In* Gap Junctions. M. V. L. Bennett and D. C. Spray, editors. Cold Spring Harbor Laboratory, Cold Spring Harbor, NY. 315–324.

Peterson, O. H., and D. Gallacher. 1987. Electrophysiology of pancreatic acinar cells. *Annu. Rev. Physiol.* 50:65–80.

Rook, M. B., H. J. Jongsma, and A. C. G. van Ginneken. 1988. Properties of single gap junctional channels between isolated neonatal heart cells. *Am. J. Physiol.* H770–H782.

Spray, D. C., A. L. Harris, and M. V. L. Bennett. 1981. Equilibrium properties of a voltage-dependent junctional conductance. *J. Gen. Physiol.* 77:77–83.

Spray, D. C., R. L. White, V. Verselis, and M. V. L. Bennett. 1985. General and comparative physiology of gap junction channels. *In* Gap Junctions. M. V. L. Bennett and D. C. Spray, editors. Cold Spring Harbor Laboratories, Cold Spring Harbor, NY. 139–153.

Spray, D. C., M. V. L. Bennett, A. C. Campos de Carvalho, B. Eghbali, A. P. Moreno, and V. Verselis. 1990. Transjunctional voltage dependence of gap junction channels. *In* Biophysics of Gap Junction Channels. C. Perrachia, editor. CRC Press, Inc., Boca Raton, FL. In press.

Stuhmer, W., F. Conti, H. Suzuki, X. Wang, M. Noda, N. Yahagi, H. Kubo, and S. Numa. 1989. Structural parts involved in activation and inactivation of the sodium channel. *Nature* (*Lond.*). 339:597–603.

Swenson, K. I., J. R. Jordan, E. C. Beyer, and D. L. Paul. 1989. Formation of gap junctions by expression of connexins in Xenopus oocyte pairs. *Cell.* 57:145–155.

Unwin, P. N. T. 1989. The structure of ion channels in membranes of excitable cells. *Neuron.* 3:665–676.

Unwin, P. N. T., and G. Zampighi. 1980. Structure of the junction between communicating cells. *Nature* (*Lond.*). 283:545–549.

Verselis, V. K., and P. R. Brink. 1984. Voltage clamp of the earthworm septum. *Biophsy. J.* 45:147–150.

Verselis, V. K., R. L. White, D. C. Spray, and M. V. L. Bennett. 1986. Gap junctional conductance and permeability are linearly related. *Science* (*Wash., DC*). 234:461–464.

Verselis, V. K., R. L. White, D. C. Spray, and M. V. L. Bennett. 1987. Induced asymmetry of gating of gap junctions in amphibian blastomeres. *J. Cell Biol.* 105:309a. (Abstr.)

Verselis, V. K., M. V. L. Bennett, and T. A. Bargiello. 1990. Complex voltage dependence of gap junctional conductance in *Drosophila*. *Biophys. J.* 57:247a. (Abstr.)

White R. L., D. C. Spray, A. C. Campos de Carvalho, B. A. Wittenberg, and M. V. L. Bennett. 1985. Some electrical and pharmacological properties of gap junctions between adult ventricular myocytes. *Am. J. Physiol.* 249:C447–455.

Zhang, J. T., and B. J. Nicholson. 1989. Sequence and tissue distribution of a second protein of hepatic gap junctions, Cx 26, as deduced from its cDNA. *J. Cell Biol.* 109:3391–3401.